

Magnetic Field Dynamics during Intense Laser Channeling in Underdense Plasma

Contact asmyth45@qub.ac.uk

A.G. Smyth, G. Sarri, D. Doria, S. Kar M. Borghesi
Centre for Plasma Physics, School of Mathematics and Physics,
The Queen's University of Belfast.
University Road, Belfast, BT7 1NN, United Kingdom.

E. Higson, J. Swain, K. Tang, J. Weston, P. Zak
Department of Physics, University of Oxford.
Parks Road, Oxford OX1 3PU, United Kingdom.

Y. Amano, H. Habara, K.A. Tanaka
Graduate School of Engineering Osaka University.
Suita, Osaka, 5650871, Japan.

M. Skramic
Trinity College, University Cambridge.
Cambridge, CB2 1TQ, United Kingdom.

Introduction

The interaction of an intense laser pulse with low-density plasma is a subject of great interest, since it sits at the core of many fundamental practical applications. These applications include electron acceleration¹, ion acceleration² and the production of high energy X-Rays³. Another high profile application for high intensity laser-plasma interactions is inertial confinement fusion (ICF) and in particular fast ignition (FI)^{4,5}. This is a form of ICF that separates the steps of compression and ignition. A deuterium-tritium fuel pellet is symmetrically irradiated, either by laser pulses or X-Rays via a hohlraum, which causes the outer layer of the fuel to ablate. For momentum to be conserved this means that the interior of the fuel must contract leading to a compressed fuel core surrounded by a diffuse coronal plasma. Ignition requires local energy deposition into the compressed core. This local position is known as a hotspot⁵ and when it reaches a sufficiently hot temperature fusion burning initiates. This burn rapidly spreads throughout the rest of the fuel and in doing so generates energy. One option for heating the hotspot is to fire a beam of suprathermal electrons into the core. However, one of the problems with FI is that to reach the core whatever heating source is being used must pass through the coronal plasma, attenuating as it travels.

One option to overcome this problem is to create a voided laser channel through the coronal plasma to create an unobstructed path to the core⁶. It has been observed that this method is also capable of producing a relativistic electron current along the channel's axis which may produce electrons suitable for the creation of a hotspot. We report here on an experiment aimed to investigate channel formation following intense laser propagation in underdense plasmas. Particular attention was paid to the magnetic field dynamics, which can provide indirect information on electron currents generated within the channel.

Experimental Setup

The experiment was conducted at the Rutherford Appleton Laboratory (RAL) in Oxfordshire. The VULCAN Nd-glass laser system was used providing 2 chirped pulse amplified (CPA⁷) beams; one incident upon a supersonic deuterium gas jet and one incident upon a 25 μm Au foil. Both pulses possessed a wavelength of 1053 nm. The interaction pulse

H. Nakamura, G. Hicks, Z. Najmudin
Blackett Laboratory, Imperial College London.
Prince Consort Road, London, SW7 2BZ, United Kingdom.

M. Vranic, E. Guillaume, J. Vieira, L.O. Silva
GoLP/Instituto de Plasma e Fusão Nuclear – Laboratório
Associado, Instituto Superior Técnico.
1049-001, Portugal.

R. Bingham, R. Heathcote, R.H.H. Scott, R. Trines, P.A. Norreys
STFC Rutherford Appleton Laboratory.
Didcot, Oxon OX11 0Qx, United Kingdom.

deposited an energy of 120 J in a pulse duration of 15 ps resulting in a focused intensity of 2×10^{18} W/cm². This pulse was preceded by a lower energy pedestal with a typical intensity contrast of $\sim 10^{-7}$. The

probe pulse carried an energy of 60 J in a duration of 1 ps which resulted in an on focus intensity of 2×10^{19} W/cm².

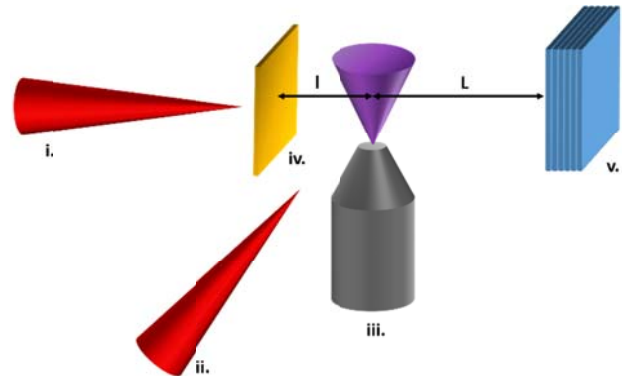


Figure 1: Schematic diagram of the experimental setup. (i.) The probe pulse. (ii.) The interaction pulse. (iii.) Supersonic gas jet (1.3 bar deuterium, $n_e \sim 10^{19}$ cm⁻³). (vi.) 25 μm Au foil. (v.) RCF stack. The two distances, l and L are 0.6 cm and 4.5 cm respectively.

The focused probe pulse interacted with the Au foil and produce a beam of protons via the TNSA⁸ mechanism. This mechanism creates a beam of multi-energetic protons which are used to probe the structures which form within the deuterium plasma via the proton probing imaging (PPI) technique⁹. The energetic range of the protons means that there is also a range of velocities. This allows temporal, as well as spatial, resolution in diagnosing the plasma when used in conjunction with a radiochromic film (RCF) stack.

Experimental Results

The RCFs showed a proton accumulation structure with three components: a dark central region running along the channel's axis and two fainter regions, one on either side of the centre. Due to the low density of the medium, the structures observed in the radiograph must be associated with electromagnetic fields. The fainter lines on either side of the

axis can be associated with the channel's walls, as observed, for example, in Sarri *et al.* These structures appear due to the ponderomotive force. The force is proportional to the square of the gradient of the laser's electric field (i.e. $\mathbf{F} \propto \nabla E^2$) meaning that charged particles that lie on either side of the centre of the pulse will experience an outwardly directed pressure. These

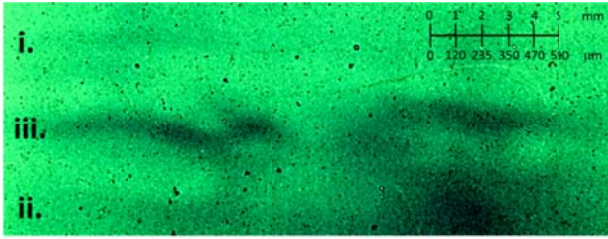


Figure 2: RCF layer showing the channel structure observed. Three regions of proton accumulation are identified in the image. The radiograph layer shown is 120ps after the peak of the laser enters the plasma.

particles bunch together at the peripheries of the pulse and form the channel walls. Similarly, particles in the centre of the laser's path will see no or virtually no gradient to the electric field and hence will remain, unperturbed, in the centre.

PIC Simulations

2D PIC simulations were ran in order to understand the processes occurring during and after laser channeling occurs. They simulated a scaled down version of the interaction using a 5 ps laser pulse and running for 25 ps. They provided information about the electromagnetic fields within the channel but also indicated that the dark central region of proton accumulation observed on the RCF was in fact due to the remnant of an azimuthal magnetic field induced by an electron current. The current was formed by the acceleration of the electrons left unperturbed along the channel's axis. Electron trajectories suggests that the main mechanism of acceleration was direct laser acceleration (DLA¹⁰).

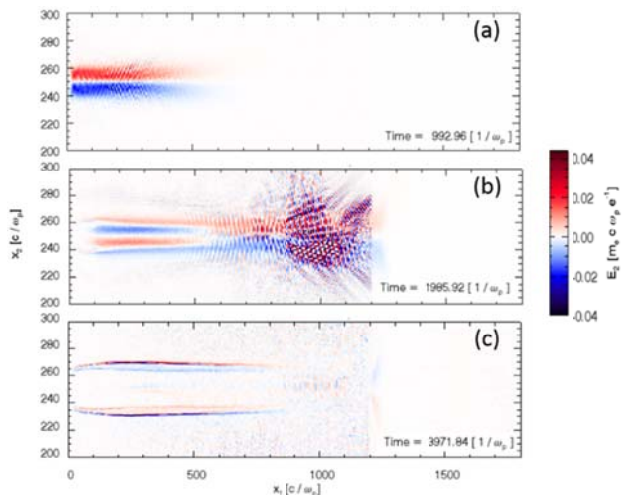


Figure 3: Evolution of the electric fields within the channel before (a & b) and after (c) the laser has left the system. The field lines in (c) correspond with the channel walls.

Particle Tracing

To confirm the topology and amplitudes of the fields created during channel formation a particle tracer was used. An electric field similar to that found in Sarri *et al.*¹¹ was used. An azimuthal magnetic field was entered into the particle tracer also. It had the form

$$\mathbf{B}_\phi = B_0 \left[e^{\left(\frac{\rho-r_B}{L_r}\right)^2} - e^{\left(\frac{\rho+r_B}{L_r}\right)^2} \right]$$

where, B_0 , is the peak magnetic field, ρ , is the radial co-ordinate of the channel, r_B , is distance between the channel/field axis and the peak of the field and L_r is the width (FWHM) of the field. This equation allowed the particle traces to match the magnitudes of the parameters used in the simulated data very well (Figure 4).

Electric field parameters of $E_{\text{peak}} \sim 2 \times 10^7 \text{ Vm}^{-1}$ and $r_E \sim 180 \mu\text{m}$ were used. For the magnetic field, $B_0 \sim 0.5 \text{ MG}$, $r_B \sim 60 \mu\text{m}$ and $L \sim 50 \mu\text{m}$ were used. These values reproduced the experimentally observed data extremely well (Figure 4).

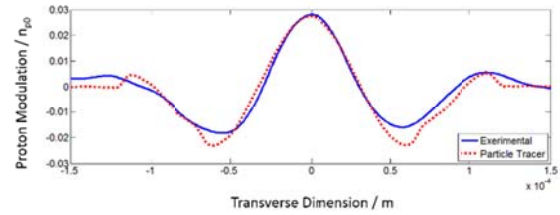


Figure 4: Comparison of the proton modulation for the experimentally observed data (solid blue) and the particle tracer data (dashed red).

Figure 5 shows the values for the parameters obtained for three consecutive RCF layers and the comparison with the values obtained from the PIC simulations. As is clear from the image the matching is extremely close.

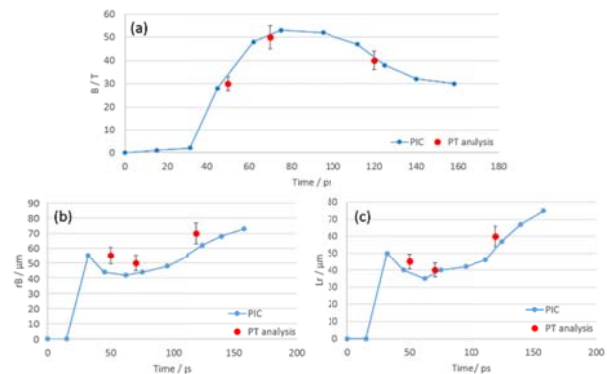


Figure 5: Comparison of (a) B_0 , (b) r_B and (c) L_r between the PIC simulations (blue line) and the particle Tracings (red points).

Taking the curl of the peak magnetic field yields a current density of $\mathbf{J} \sim 10^{12} \text{ Am}^{-2}$. Assuming that the electrons comprising the current were relativistic (i.e. $v_e \sim c$) reveals that the magnetic field was induced by an relativistic electron current of $I \sim 15 \text{ kA}$ which corresponds to an electron density of $n_e \sim 10^{16} \text{ cm}^{-3}$.

Conclusions

Presented here were measurements of the magnetic field produced during laser driven channel formation with a uniform density plasma ($n_e \sim 10^{18}$) conducted at the VULCAN laser facility. The magnetic field is consistent with generation by an electron current which is established along the centre of the channel. Values for the magnetic field properties were obtained by conducting particle tracing analysis matched against radiochromic films and backed up by 2D PIC simulations.

It was seen that a peak magnetic field of 0.5 MG was achieved. Using the trapped magnetic field observed and measured it was found that a peak relativistic electron current of ~ 15 kA with an electron density of $\sim 10^{16}$ cm⁻³ was produced along the centre of the channel. PIC simulations suggest that this current was produced mainly via direct laser acceleration of electrons.

Measurement of the azimuthal magnetic field formed during channelling as a means of measuring the electron current produced has shown that a sizable density of collimated, relativistic electrons can be produced. The possible impact of this on Hole Boring Fast ignition schemes will need to be carefully assessed.

References

1. Esarey, E., Schroeder, C. & Leemans, W. Physics of laser-driven plasma-based electron accelerators. *Rev. Mod. Phys.* **81**, 1229–1285 (2009).
2. Willingale, L. *et al.* Collimated Multi-MeV Ion Beams from High-Intensity Laser Interactions with Underdense Plasma. *Phys. Rev. Lett.* **96**, 245002 (2006).
3. Kneip, S. *et al.* Bright spatially coherent synchrotron X-rays from a table-top source. *Nat. Phys.* **6**, 980–983 (2010).
4. Atzeni, S. Inertial fusion fast ignitor: Igniting pulse parameter window vs the penetration depth of the heating particles and the density of the precompressed fuel. *Phys. Plasmas* **6**, 3316–3326 (1999).
5. Tabak, M. *et al.* Review of progress in Fast Ignition. *Phys. Plasmas* **12**, 057305 (2005).
6. Borghesi, M. *et al.* Relativistic Channeling of a Picosecond Laser Pulse in a Near-Critical Preformed Plasma. *Phys. Rev. Lett.* **78**, 879–882 (1997).
7. Strickland, D. & Mourou, G. Compression of amplified chirped optical pulses. *Opt. Commun.* **55**, 447–449 (1985).
8. Macchi, A., Borghesi, M. & Passoni, M. Ion acceleration by superintense laser-plasma interaction. *Rev. Mod. Phys.* **85**, 751–793 (2013).
9. Romagnani, L. Laser Plasma Investigations Employing Laser-Driven Proton Probes. *PhD Thesis, Queen's Univ. Belfast* (2005).
10. Gahn, C. *et al.* Multi-MeV Electron Beam Generation by Direct Laser Acceleration in High-Density Plasma Channels. *Phys. Rev. Lett.* **83**, 4772–4775 (1999).
11. Sarri, G. *et al.* Creation of persistent, straight, 2 mm long laser driven channels in underdense plasmas. *Phys. Plasmas* **17**, 113303 (2010).